Chapter 13
Conditions for Obtaining Good Impedances

EIS has a great advantage in comparison with other electrochemical techniques because it permits one to validate experimental data, that is, to determine whether obtained data are good [1]. This property arises from Cauchy's integral theorem [3, 554] implying a relation between the real and imaginary components of a complex function. Kramers [555, 556] and Kronig [557] introduced transformations allowing one to calculate the imaginary part from the real part and the real part from the imaginary impedance component. They applied it first to optics. In experimental impedance measurements, if the results obtained from the transformations agree with the experimental data, then one can state that the data are formally correct and are Kramers-Kronig compliant.

13.1 Kramers-Kronig Relations

The Kramers-Kronig relations allow one to calculate the real part of a complex function from the imaginary part and the imaginary part from the real part only. They were initially applied to electrical impedances by Bode [558] and further discussed and applied to EIS [559–568]. To satisfy Kramers-Kronig relations, the complex function must satisfy four criteria, as follows [223, 559–561]:

1. *Linearity:* a system is linear when its response to a sum of individual input signals is equal to the sum of the individual responses: $L(af_1 + bf_2) = aL(f_1) + bL(f_2)$. This condition implies that the system is described by a system of linear differential equations. Electrochemical systems are usually highly nonlinear, and the impedance is obtained by linearization of equations using small amplitudes of the applied perturbation. In addition, for linear systems responses are independent of the amplitude. This condition can be easily verified experimentally: one should decrease the applied amplitude twice and compare the results. If the obtained impedance is the same, the system is linear.

A. Lasia, *Electrochemical Impedance Spectroscopy and its Applications*,
DOI 10.1007/978-1-4614-8933-7_13,

2. *Causality:* the response of a system must be entirely determined by the applied perturbation, that is, the output depends only on the present and past input values. A causal system cannot predict its future because its future is determined by the past events. This also means that the system does not generate noise independently of the applied signal for $t \geq 0$. Causal systems are called physically realizable systems. If a system is at rest and a perturbation is applied at $t = 0$, then the response must be constrained for $\omega \to 0$. In addition, the response must be zero at $\omega \to \infty$. However, in electrochemical systems, a weaker condition can be applied requiring that the transfer function be bounded.
3. *Stability:* the stability of a system is determined by its response to inputs. A stable system remains stable until excited by an external source, and it should return to its original state once the perturbation is removed, that is, the system cannot supply power to the output irrespective of the input. In other words, the total energy generated by the system cannot exceed the total input energy. A consequence of this condition is that the transfer function is bounded, i.e., $|Z(\omega)|^2 < A$, where A is a constant. A system is stable if its response to the impulse excitation approaches zero after a long time or when every bounded input produces a bounded output. The impedance $Z(s)$ must satisfy the following conditions: $Z(s)$ is real when s is real (that is, when $\omega \to 0$) and $\mathrm{Re}[Z(s)] \geq 0$ when $\nu \geq 0$ (where $s = \nu + j\omega$). This last condition ensures that there are no negative resistances in the system. Impedance measurements must also be stationary, that is, the measured impedance must not be time dependent. This condition may be easily checked by repetitive recording of the impedance spectra and comparison of the obtained results, which should be identical.
4. *Finiteness:* this condition was already implied earlier. It means that the real and imaginary components of the impedance must be finite-valued over the entire frequency range $0 < \omega < \infty$. In particular, the impedance must tend to a constant real value for $\omega \to 0$ and $\omega \to \infty$.

Although these relations will be written below for impedances they also hold for admittances and other complex transfer functions. Assuming that all the aforementioned conditions are met, the Kramers-Kronig relations are obtained allowing the calculation of the imaginary impedance from the real part:

$$Z''(\omega) = -\left(\frac{2\omega}{\pi}\right)\int_0^\infty \frac{Z'(x) - Z'(\omega)}{x^2 - \omega^2}\mathrm{d}x \tag{13.1}$$

and the real from the imaginary:

$$Z'(\omega) = Z'(\infty) + \frac{2}{\pi}\int_0^\infty \frac{xZ''(x) - \omega Z''(\omega)}{x^2 - \omega^2}\mathrm{d}x, \tag{13.2}$$

$$Z'(\omega) = Z'(0) + \int_0^\infty \frac{\left(\frac{\omega}{x}\right)Z''(x) - Z''(\omega)}{x^2 - \omega^2}\mathrm{d}x. \tag{13.3}$$

There are also similar relations for the phase angle and modulus [3]:

$$\varphi(\omega) = \left(\frac{2\omega}{\pi}\right)\int_0^\infty \frac{\ln|Z(x)|}{x^2 - \omega^2}\mathrm{d}x, \tag{13.4}$$

$$\ln|Z(\omega)| = \frac{2}{\pi}\int_0^\infty \frac{\varphi(x)}{x - \omega}\mathrm{d}x. \tag{13.5}$$

Several other forms of these relations can be found in the literature [3]. Although the preceding equations were written for impedances, *they are valid for any complex transfer function*. Kramers-Kronig relations are very restrictive, and in EIS some of them might be slightly relaxed, and instead of the impedances, the admittances can be used. This will be discussed in what follows.

Kramers-Kronig relations demand integration in a wide frequency range from zero to infinity, which is experimentally impossible. They are also sensitive to stochastic errors, ε, and the average value of the errors of the real, ε', and imaginary, ε'', parts must be equal to zero as well as the average value of the integral [273]:

$$\mathrm{E}\left\{\frac{2\omega}{\pi}\int_0^\infty \frac{\varepsilon'(x)}{x^2 - \omega^2}\,\mathrm{d}x\right\} = 0. \tag{13.6}$$

Various methods have been proposed to carry out Kramers-Kronig transformations in practice; they are described in what follows.

13.1.1 Polynomial Approximation

One method is to approximate real and imaginary impedances as functions of the frequency by polynomials in ω [560, 561, 568, 569],

$$Z(\omega) = a_0 + a_1\omega + a_2\omega^2 + a_3\omega^3 + \ldots = \sum_{i=0}^{n} a_i\omega^i, \tag{13.7}$$

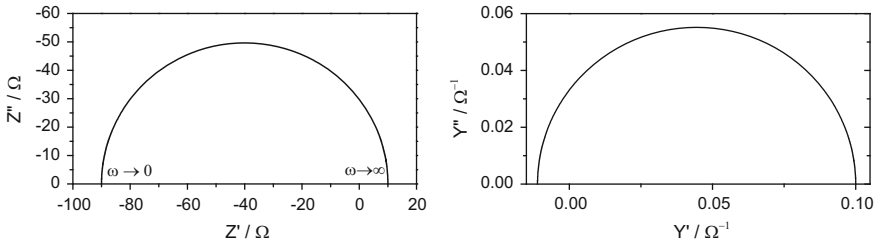

Fig. 13.1 Complex plane impedance and admittance plots for circuit in Fig. 2.34 with $R_s = 10\,\Omega$, $C = 10^{-5}$ F, and $R = -100\,\Omega$

or log ω [564],

$$Z(\omega) = a_0 + a_1 \log\omega + a_2 (\log\omega)^2 + a_3 (\log\omega)^3 + \ldots = \sum_{i=0}^{n} a_i \ (\log\omega)^i, \quad (13.8)$$

and subsequent integration of the polynomials using Eqs. (13.1), (13.2), and (13.3). Approximation by splines can also be used. However, there are two problems with this integration. First of all, integrations should be carried out in a frequency range from zero to infinity. Because experimental data are acquired in a limited frequency range, extrapolation must be carried out outside the experimental limits. In certain cases (e.g., one or two semicircles), one knows these limits and the extrapolation is easier. However, in some cases one does not know how the impedance should behave outside the experimental range, and the extrapolation might be doubtful. Integration in a more narrow frequency range could lead to significant errors [570]. Approximation by splines is not well suited for extrapolation outside the experimental frequency range.

Another problem is related to the discontinuity of the integrated function at $x = \omega$. Several authors have proposed a distribution of $1/(x^2 - \omega^2)$ in series around the point $x = \omega$ and an integration of the sum of the elements [560, 561, 563, 570].

Although in principle Kramers-Kronig relations demand that the impedance have a finite value at $\omega = 0$ and $\omega \to \infty$, it has been shown that the CPE

$$\hat{Z} = \frac{1}{(j\omega)^{\phi} T} \quad (13.9)$$

transforms correctly for $-1 \leq \phi \leq 1$, including the Warburg impedance ($\phi = 0.5$) [561, 563, 571].

System with negative resistance cannot be represented by a passive circuit with positive R, L, and C elements. The stability criterion demands that there be no negative impedances in the system (rule 3 of Kramers-Kronig conditions). For example, the system shown in Fig. 13.1 contains negative resistance, and its impedance is not transformable. However, Kramer-Kronig transforms can also be applied to admittances. Admittance calculated for this case is also shown in Fig. 13.1, and it is perfectly Kramers-Kronig transformable. Moreover, infinite impedance corresponds to zero admittance which is transformable. This topic will be further discussed in Sect. 13.3.4.

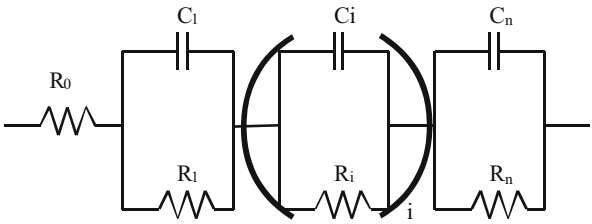

Fig. 13.2 Voigt circuit consisting of $n(RC)$ elements

13.1.2 Checking Kramers-Kronig Compliance by Approximations

It is possible to replace the Kramers-Kronig integration by approximation. If the system can be well approximated by a linear circuit, then it must be Kramers-Kronig transformable. Orazem and coworkers [572, 573] proposed using the Voigt circuit displayed in Fig. 13.2.

Each element of this circuit consists of the connection of R and C in parallel, and it is, of course, transformable; therefore, their sum is also transformable. The impedance of the Voigt circuit is described by the following equation:

$$\hat{Z} = R_0 + \sum_{i=1}^{n} \frac{R_\mathrm{i}}{1 + j\omega\tau_\mathrm{i}} \tag{13.10}$$

where $\tau_i = R_\mathrm{i}C_\mathrm{i}$ is the time constant of element i of the circuit. Using a sufficient number of such elements the CPE or Warburg elements can also be approximated [572]. To approximate circuits containing inductances, negative values of R_i may be used keeping the time constants positive [572]. The number of Voigt elements necessary for a correct approximation depends on the system random errors: the greater the errors, the smaller the number of necessary elements.

Boukamp and Macdonald [574] and Boukamp [575] proposed fitting impedances to a Voigt circuit with a fixed distribution of time constants, taking six to seven time constants per decade or simply the time constant equal to the inverse of the experimental frequency ω_i, $\tau_\mathrm{i} = 1/\omega_\mathrm{i}$; in the latter case, a perfect approximation is obtained even in the presence of the experimental noise, which should, in principle, be avoided. By fixing the values of τ_i, the only unknown parameters in Eq. (13.10) are R_i. The CNLS approximation becomes linear and no initial guess of parameters R_i is necessary (Chap. 14). The approximating function becomes

$$\begin{aligned} \hat{Z}(\omega_\mathrm{k}) &= R_0 + \sum_{i=1}^{n} \frac{R_\mathrm{i}}{1 + j\omega_\mathrm{k}\tau_\mathrm{i}} = \\ &= R_0 + \sum_{i=1}^{n} \frac{R_\mathrm{i}}{1 + (\omega_\mathrm{k}\tau_\mathrm{i})^2} - j\sum_{i=1}^{n} \frac{\omega_\mathrm{k}\tau_\mathrm{k}R_\mathrm{i}}{1 + (\omega_\mathrm{k}\tau_\mathrm{i})^2}. \end{aligned} \tag{13.11}$$

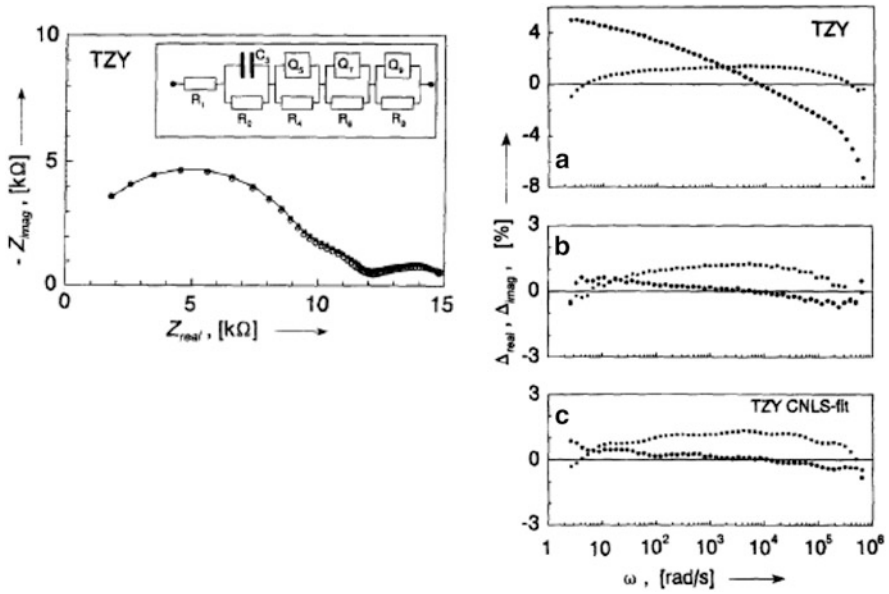

Fig. 13.3 Example of experimental data for solid electrolyte that are not Kramers-Kronig transformable, *left*, and residual plots: (**a**) real to imaginary and imaginary to real, (**b**) relative errors of complex transformation, and (**c**) errors of CNLS fit to model in (**a**); *circles*: real-to-imaginary; *squares*: imaginary-to-real transformations (From Ref. [575] Reproduced with permission of Electrochemical Society)

In the approximation, Boukamp suggested using modulus weighting. Moreover, in some cases it might be necessary to add inductance or capacitance in series with R_0. Boukamp [575] presented an example of non-Kramers-Kronig-transformable data analyzed by CNLS fit (Fig. 13.3), where the symbol Q_i denotes a CPE. It is not evident from the complex plane plot if the impedance data are really transformable. To answer this question, the residual plots of the real and imaginary impedances, $\Delta = Z_{exp} - Z_{transformed}$, should be inspected. They are also presented in Fig. 13.3. It is evident that the differences are systematic, not random, and cannot be ascribed to random errors. This means that the impedance in Fig. 13.3a is not Kramers-Kronig transformable. In fact, it was found that steady state was not reached in the experiment, and the material properties changed with time.

In the case of blocking electrodes, the impedance increases to infinity as the frequency approaches zero. In such cases, approximation with the Voigt circuit is not appropriate. When a high-frequency impedance is finite, the easiest way to verify the Kramers-Kronig compliancy is to fit the impedances to the admittance representation of the circuit containing a ladder of (RC) element series (Fig. 13.4) [575]. In addition, capacitance, C_0, or inductance can be added in parallel.

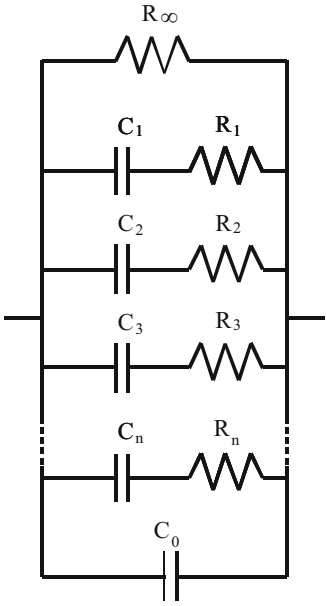

Fig. 13.4 Circuit proposed for fitting admittance of blocking electrodes

The admittance of this circuit at a frequency ω_k is

$$\hat{Y}(\omega_k) = \frac{1}{R_\infty} + \sum_{i=1}^{n} \frac{1}{R_i + \dfrac{1}{j\omega_k C_i}} + j\omega_k C_0 = \\ = \frac{1}{R_\infty} + \sum_{i=1}^{n} \frac{\omega_k^2 \tau_i C_i}{1 + (\omega_k \tau_i)^2} + j\left(\sum_{i=1}^{n} \frac{\omega_k C_i}{1 + (\omega_k \tau_i)^2} + \omega_k C_0 \right), \tag{13.12}$$

where the values of ω_k are predefined (six to seven per decade). An example of such a test is shown in Fig. 13.5. Fewer than seven time constants per decade are necessary to approximate well the experimental admittances.

The conditions necessary for the Kramers-Kronig transform demand that the resistances be all positive. The values of R_i might be negative, but the corresponding C_i must also be negative to produce positive values of time constants [304]. However, in experimental work, negative dynamic impedances may appear, although they might lead to a stable dynamic response (see subsequent discussion on the Nyquist criterion of stability). Boukamp [575] suggested that to avoid this problem, one could add computationally a parallel resistance to the dispersion data so that the negative resistance is removed completely. An example of such an operation is displayed in Fig. 13.6. It is evident from plot b that the computational addition of the parallel resistor of 400 Ω eliminates negative resistance. However, such a procedure is not necessary, as shown in Sect. 13.3.4.

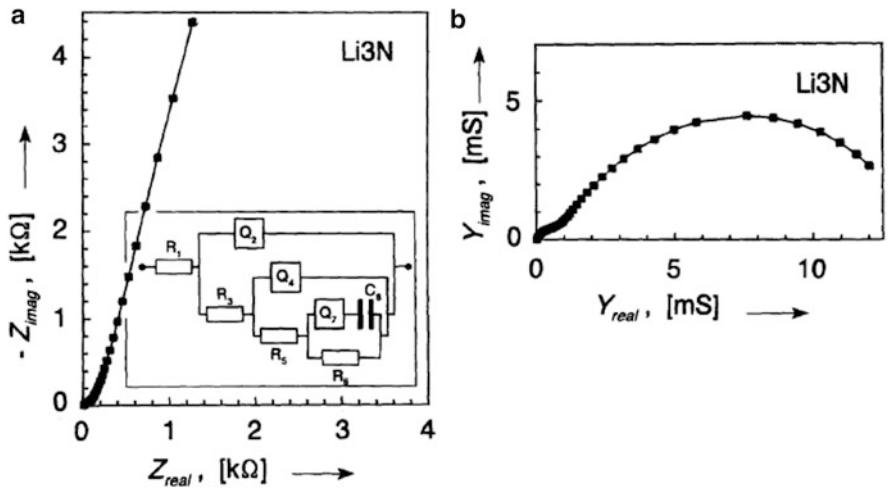

Fig. 13.5 Complex plane impedance and admittance plots for hydrogen-doped Li_3N monocrystals; (**a**) impedance plot and fit to model indicated in *inset*; (**b**) admittance plot and fit to Eq. (13.12); points experimental, line fits (From Ref. [575] Reproduced with permission of Electrochemical Society)

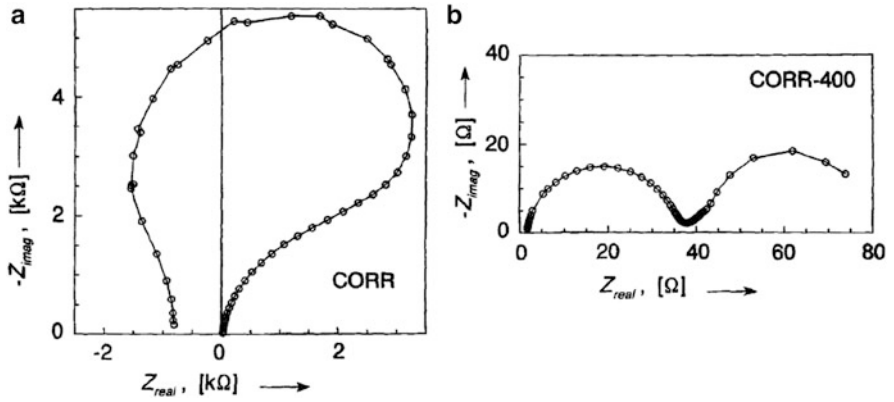

Fig. 13.6 Impedance of corroding Cr electrode; (**a**) experimental data, (**b**) experimental data with computational addition of parallel resistance of 400 Ω (From Ref. [575] Reproduced with permission of The Electrochemical Society)

Analysis of the plot in Fig. 13.6b using linear approximation, Eq. (13.11), is displayed in Fig. 13.7. Note that important deviations appear at $\omega > 10^3$ rad s^{-1}. In further analysis, these data points were eliminated without any important loss of information in the high-frequency zone in Fig. 13.6a [575].

It should be stressed that approximations by Eq. (13.11) or Eq. (13.12) are used only for testing the compliance with the Kramers-Kronig transforms, and the parameters found have no physical meaning.

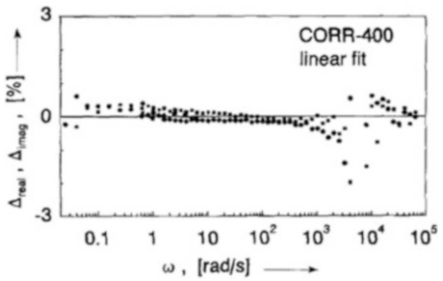

Fig. 13.7 Relative residuals for complex linear fit of data in Fig. 13.6b using 7.6 time constants per decade (From Ref. [575] Reproduced with permission of Electrochemical Society)

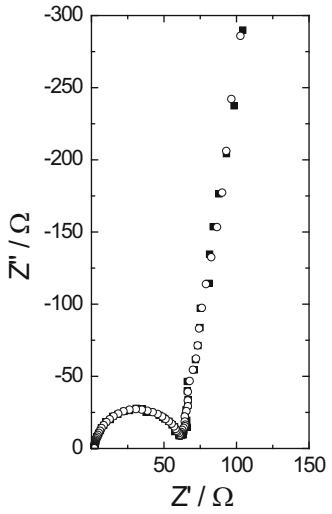

Fig. 13.8 Original (*squares*) and transformed (*open circles*) data in noise data file

Boukamp has prepared a simple and easy-to-use program, KKtest, which uses Eq. (13.11) or Eq. (13.12) to check the validity of data. It is available on the Internet [576] and presented in Example 13.1 (see also Exercise 13.2 and 13.3).

Example 13.1 Check the Kramers-Kronig compliance of the data including noise and including drift using KKtest. A comparison of the original data with added random noise and KK transformed data is displayed in Fig. 13.8. Transformed data display no systematic differences from the original data, and one can say that the data are Kramers-Kronig compliant. The same may also be observed on the differences graph also displayed in the KKtest program.

Next the data drift should be analyzed. A comparison of the original and transformed data is shown in Fig. 13.9. It is evident that the original and transformed data are very different, which means that the original data are not Kramers-Kronig compliant and cannot be used for further analysis. Such systematic deviations are also observed on the difference graphs, see Exercises 13.2 and 13.3.

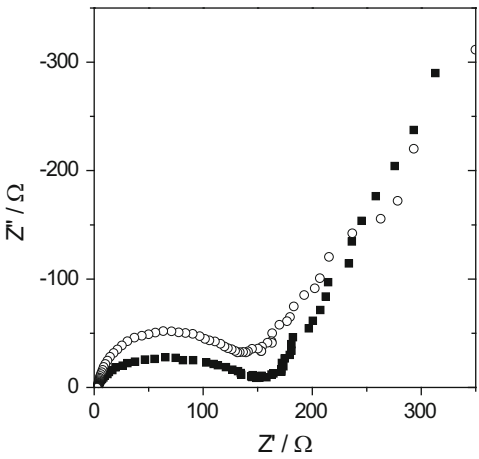

Fig. 13.9 Original (*squares*) and transformed (*open circles*) data in drift data file

13.2 Linearity

The linearity of the observed impedance is directly related to the amplitude of the ac signal applied to the system. Electrochemical systems are intrinsically nonlinear, and a sufficiently small amplitude is necessary to linearize such systems. Smith [29] suggested using an amplitude of $\leq 8/n$ mV peak to peak. A more detailed analysis was performed by Hirschorn et al. [577] and Hirschorn and Orazem [578] taking into account differences in the transfer coefficients and solution resistance. Assuming a simple model of the redox system without diffusion (Fig. 4.2) that is with negligible mass transfer impedance Z_W, the maximum ac voltage amplitude causing an error of $\leq$0.5 % is [577]

$$\Delta E = 0.2\sqrt{\frac{k_f b_f + k_b b_b}{k_b b_f^3 + k_b b_b^3}\left(1 + \frac{R_s}{R_{t,obs}}\right)}, \tag{13.13}$$

where $b_i = \alpha_i nf$, α_i is the transfer coefficient, n is the number of electrons exchanged, $f = F/RT$, the indices f and b indicate forward and backward reactions, respectively, R_s is the solution resistance, and $R_{t,obs}$ is the charge transfer resistance. Because of the solution resistance, the actual potential applied to the electrode is lower than that used by the instrument, and this value depends on the frequency. For a case where the transfer coefficient $\alpha_f = 0.5$ and assuming $R_s \ll R_{t,obs}$ and $k_f = k_b$, the maximum amplitude for $n = 1$, ΔE, is 10 mV, while for $\alpha_f = 0.2$ it is 7.1 mV and depends on the slope of the current-potential curve. At high frequencies, the circuit reduces to a simpler ($R_s C_{dl}$) model, and a characteristic frequency for the transition from low- to high-frequency behavior is [578]

$$f_t = \frac{1}{2\pi R_{t,obs} C_{dl}} \left(1 + \frac{R_{t,obs}}{R_s}\right). \tag{13.14}$$

Application of Kramers-Kronig transforms reveals that they are not very sensitive to system nonlinearities [561]. Experimentally, nonlinearity affects the charge transfer resistances, which decrease with increases in the amplitude [561, 578–580]. However, it has been shown that when the experimental frequency passes through the transition frequency, Eq. (13.14), the Kramers-Kronig transforms will be affected by the nonlinearity of the system.

It seems that the simplest way to check for nonlinearity is to take measurements at different amplitudes and compare the obtained impedances, which should be identical for linear systems. In general, a 5 mV amplitude is recommended; however, in certain conditions, it might be different; Eq. (13.13) gives a good indication in simple conditions, but more information about the system kinetics is necessary.

13.3 Stability

13.3.1 Drift

One of the biggest problems in impedance measurements is related to changes in a system with time. This effect appears when surface conditions or electrode contamination evolves with time. An example of a corroding system in which a slow potential sweep was applied during the experiment is displayed in Fig. 13.10. This potential sweep simulates changes in the surface conditions of the corroding electrode. A Kramers-Kronig transform easily detects such changes. Transforms of

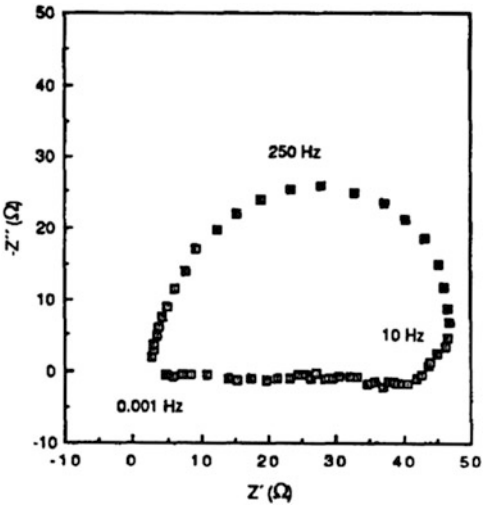

Fig. 13.10 Impedance of corroding iron electrode with superimposed potential sweep of 0.133 mV s^{-1} (From Ref. [561], copyright (1990), with permission from Elsevier)

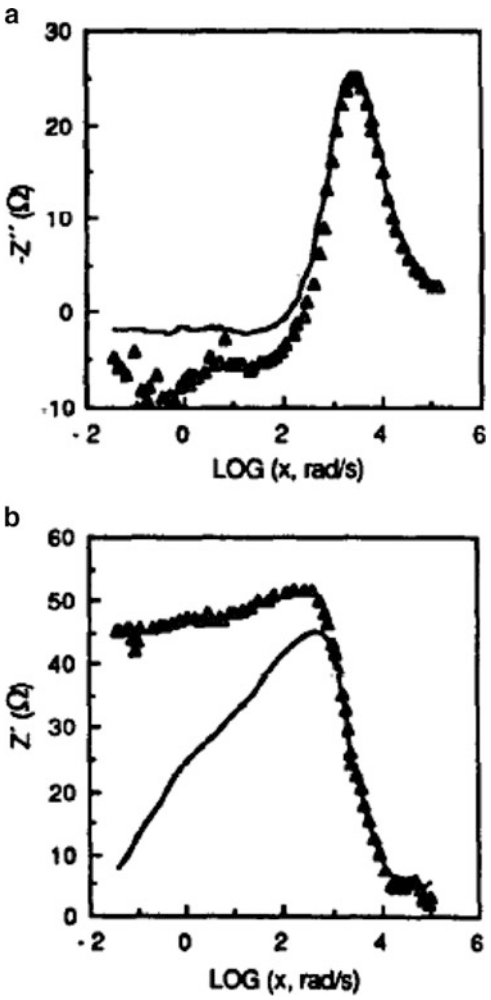

Fig. 13.11 Kramers-Kronig transforms, (**a**) real to imaginary and (**b**) imaginary to real, of data in Fig. 13.10 (From Ref. [561], copyright (1990) with permission from Elsevier)

the experimental data in Fig. 13.10 are shown in Fig. 13.11. At low frequencies, which take much more time during measurements, strong deviations are observed. The influence of drift was recently simulated and discussed [579].

An odd harmonic test [125, 580] was also proposed in the literature to check system linearity.

13.3.2 Dealing with Nonstationary Impedances

In practice, there are often cases where impedance changes continuously with time. Such changes are observed in, for example, cases of active corrosion, fuel cell poisoning, and surface changes. In these cases, during the frequency sweep, each

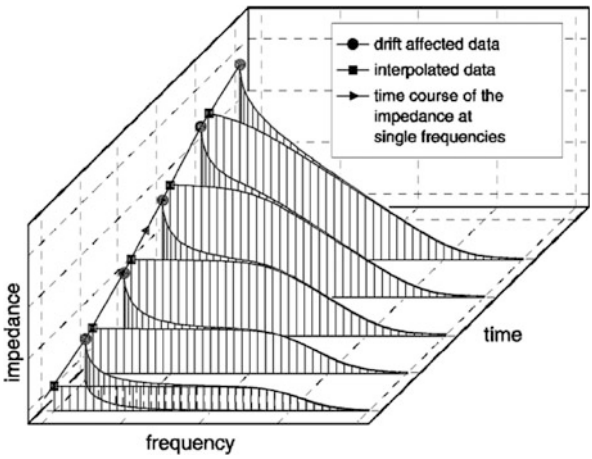

Fig. 13.12 Experimental impedance data (*circles*) and method of obtaining time-invariant impedances (*squares*) (From Ref. [585] with permission of Royal Society of Chemistry)

measurement corresponds to a new electrode state. The theoretical foundations of nonstationary systems were established by Stoynov and coworkers [581–584]; however, they were applied to simulated data only. Wagner and coworkers [585, 586] proposed a relatively simple interpolation method dealing with such systems. They recorded a series of impedance measurements at distinct time intervals, i.e., the time of each measurement at one frequency was assumed to be short and known. Then three-dimensional plots of impedance versus frequency and time were constructed (Fig. 13.12). The experimental impedances (circles) were first plotted as a function of frequency and time. Then data at each frequency were interpolated versus time (see an example of one line at the lowest frequency in Fig. 13.12), and impedances were found at a given time. This interpolation could supply impedances at various times. Such interpolation should be repeated at all frequencies. It is obvious that data at the lowest frequencies are most affected by drift because they take longer to be recorded. Such a procedure should be repeated for real/imaginary or magnitude/phase angle data. Although in general a smoothing function could be used for data interpolation at one frequency, the authors found that in their case a linear interpolation was sufficient. To further refine the obtained data, a Z-HIT transform (see Sect. 3.14) was applied, and the results from this transformation were used for analysis. An example of the results is displayed in Fig. 13.13.

13.3.3 Stability of Electrochemical Systems

In this section we will look in more detail at system stability [587]. In control system theory, a stable system is one that produces a bounded response to a bounded input. In general, system stability depends on the proprieties of the transfer function, in this case of the impedance or the admittance [588]. Impedance and

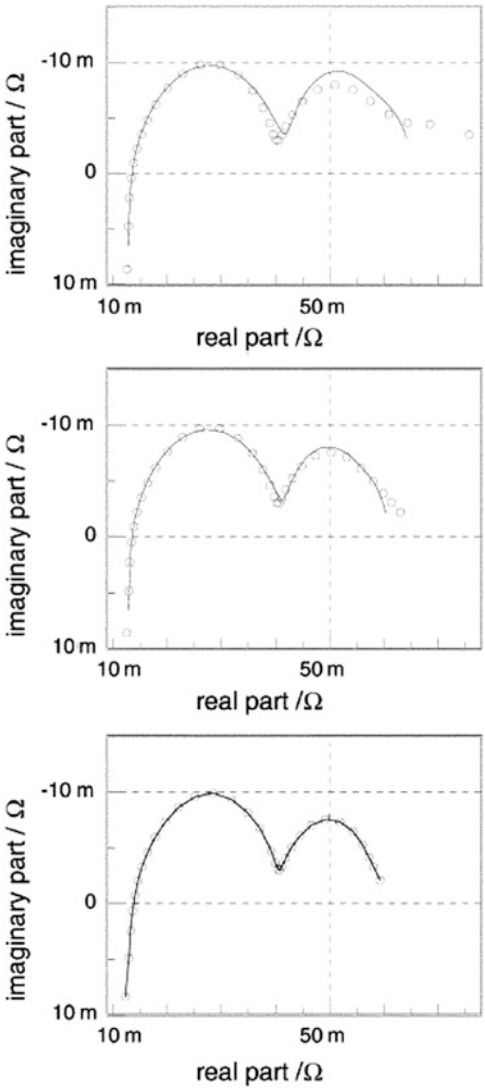

Fig. 13.13 Complex plane plots illustrating compensation of time drift for fuel cell under galvanostatic control, *top* – directly measured impedance, *middle* – after extrapolation procedure, *bottom* – after additional Z-HIT refinement; *continuous lines* – approximations (From Ref. [585] with permission of Royal Society of Chemistry)

admittance are defined as a ratio of the Laplace transforms of the potential and current:

$$\hat{Z}(s) = \frac{1}{\hat{Y}(s)} = \frac{\overline{E}(s)}{\overline{i}(s)}, \tag{13.15}$$

where the parameter $s = \sigma + j\omega$ is a complex number. Let us suppose that the potential is applied and the current is measured. Moreover, let us assume that the potential is simply Dirac's delta function, $\delta(t)$, applied at $t = 0$. Its Laplace transform is

$$L[\delta(t)] = 1\,\mathrm{V/s}, \tag{13.16}$$

and the current in the Laplace domain is

$$\overline{i}(s) = \frac{1}{\hat{Z}(s)} = \hat{Y}(s) = \frac{K\prod_{m=1}^{M}(s-\mu_{\mathrm{m}})\prod_{n=1}^{N}\left[s^2 - 2\nu_{\mathrm{n}}s + \left(\nu_{\mathrm{n}}^2 + \beta_{\mathrm{n}}^2\right)\right]}{\prod_{q=1}^{Q}\left(s-\lambda_{\mathrm{q}}\right)\prod_{r=1}^{R}\left[s^2 - 2\rho_{\mathrm{r}}s + \left(\rho_{\mathrm{r}}^2 + \omega_{\mathrm{r}}^2\right)\right]}, \tag{13.17}$$

where the admittance is represented as a ratio of two polynomials factored in linear and quadratic terms. Quadratic terms having real zeros (the delta of the quadratic equation is larger than zero) can always be presented in the form $s - \lambda_{\mathrm{q}}$; however, when delta is negative, complex roots appear. The admittance has $M + N$ zeros and $Q + R$ poles, while the impedance has $M + N$ poles and $Q + R$ zeros. The parameters μ_{m}, ν_{n}, β_{n}, λ_{q}, ρ_{r}, and ω_{r} are constants. The zeros of the admittance are

$$s = \mu_{\mathrm{m}} \quad \text{and} \quad s = \nu_{\mathrm{n}} \pm j\beta_{\mathrm{n}}, \tag{13.18}$$

and the poles are

$$s = \lambda_{\mathrm{q}} \quad \text{and} \quad s = \rho_{\mathrm{r}} \pm j\omega_{\mathrm{r}}. \tag{13.19}$$

Therefore, there are real and complex conjugated zeros and roots. Examples of such polynomials representing the impedance of a system were presented, for example, in Eq. (2.91) for an *R-C* connection, Eq. (2.94) for an *R-L* connection, and Eq. (2.97) for an *R-L-C* connection in series. This expression can be simplified into partial fractions:

$$\overline{i}(s) = \hat{Y}(s) = \frac{1}{\hat{Z}(s)} = K\left[\sum_{q=1}^{Q}\frac{A_{\mathrm{q}}}{s-\lambda_{\mathrm{q}}} + \sum_{r=1}^{R}\frac{B_{\mathrm{r}}}{s^2 - 2\rho_{\mathrm{r}}s + \left(\rho_{\mathrm{r}}^2 + \omega_{\mathrm{r}}^2\right)}\right], \tag{13.20}$$

where A_{q} and B_{r} are called residues. The inverse Laplace transform gives the dependence of the current as a function of the potential:

$$i(t) = K\left[\sum_{\mathrm{q}=1}^{Q}A_{\mathrm{q}}\exp\left(\lambda_{\mathrm{q}}t\right) + \sum_{\mathrm{r}=1}^{R}B_{\mathrm{r}}\frac{1}{\omega_{\mathrm{r}}}\exp(\rho_{\mathrm{r}}t)\sin\left(\omega_{\mathrm{r}}t\right)\right]. \tag{13.21}$$

When the poles λ_{q} are negative, the current relaxes to zero and the system is stable. In the case of complex poles, Eq. (13.19), ρ_{r} must be negative or zero, that is, the real part of the root cannot be negative to assure stability. Solutions for different values of λ_{q} and ρ_{r} are presented in Fig. 13.14. Stable systems are obtained only when these values are negative or zero. When $\lambda_{\mathrm{q}} = 0$, a time-independent constant

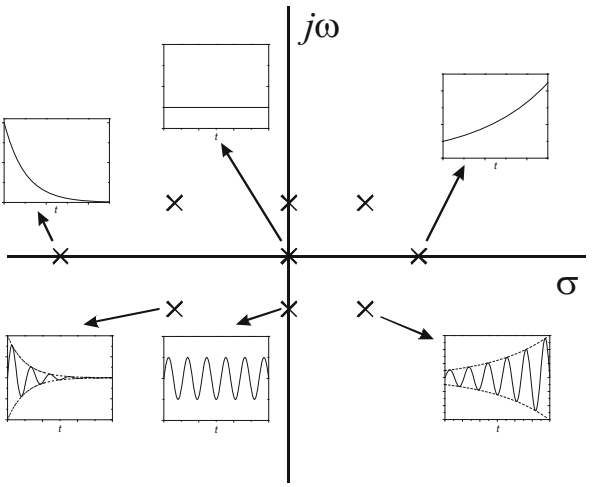

Fig. 13.14 Transients obtained for different positions and nature of poles at *s*-plane

signal is obtained, and when $\rho_r = 0$, a steady-state oscillation is produced. The poles and zeros of Eq. (13.17) are presented on the *s*-plane, where the *x*-axis is real (σ) and *y*-axis imaginary *(jω)*. System theory [587] holds that a necessary and sufficient *condition for a system to be stable is that all poles of the transfer function must have negative real parts. If some roots are positive, then the system becomes unstable as its response becomes unbounded*. The preceding conditions apply to the system transfer function, which in Eq. (13.17) is written as the admittance. However, in electrochemistry, the impedance is usually studied. Therefore, the *admittance transfer function should have all poles negative, which indicates that all zeros of the impedance should be negative*. The admittance/impedance transfer function is usually written in the form

$$\hat{Z}(s) = K \frac{\prod_{i=1}^{N_z} (s - z_i)}{\prod_{k=1}^{N_p} (s - p_i)}, \tag{13.22}$$

where there are N_z zeros z_i and N_p poles p_i. A few examples are given in what follows.

Let us consider a simple circuit $R_0(R_1C_1)$, shown in Fig. 2.26. Its impedance is described by Eq. (2.128), which can be rearranged into the following form, Eq. (13.22):

$$\hat{Z}(s) = R_0 + \frac{1}{sC_1 + \frac{1}{R_1}} = \frac{R_0\left[s + \frac{1}{C_1}\left(\frac{1}{R_0} + \frac{1}{R_1}\right)\right]}{s + \frac{1}{R_1C_1}}. \tag{13.23}$$

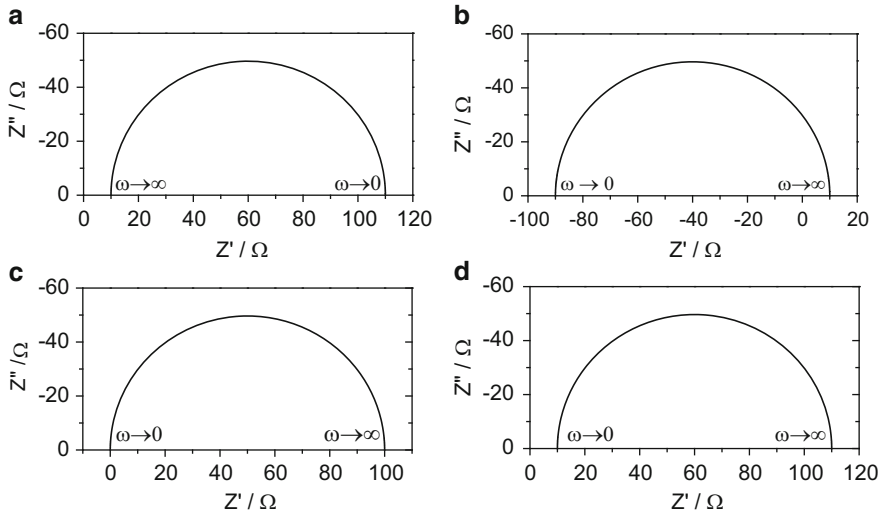

Fig. 13.15 Complex plane plots for a simple circuit $R_0(R_1C_1)$ consisting of resistance R_0 in series with parallel connection of capacitance C_1 and resistance R_1, Eq. (13.23); parameters: $C_1 = 2 \times 10^{-5}$ F, (**a**) $R_0 = 10\ \Omega$, $R_1 = 100\ \Omega$, (**b**) $R_0 = 10\ \Omega$, $R_1 = -100\ \Omega$, (**c**) $R_0 = 100\ \Omega$, $R_1 = -100\ \Omega$, (**d**) $R_0 = 110\ \Omega$, $R_1 = -100\ \Omega$

This function has one pole,

$$p = -\frac{1}{R_1 C_1}, \tag{13.24}$$

and one zero,

$$z = -\frac{1}{C_1}\left(\frac{1}{R_0} + \frac{1}{R_1}\right). \tag{13.25}$$

If all circuit parameters are positive, then the pole and zero are negative and the system is stable. For the impedances in Fig. 13.15 the poles and zeros are displayed on the *s*-plane in Fig. 13.16. When all the circuit parameters are positive, the poles and zeros are always negative. The complex plane plot in this case, which displays well known behavior, is shown in Fig. 13.15a.

Let us now assume that $R_{ct} < 0$. There are a few different cases, depending on the relative values of R_0 and R_1.

When $R_0 < -R_1$, the zero-frequency impedance is negative, $R(\omega = 0) = R_0 + R_1 < 0$, the complex plane plot is shown in Fig. 13.15b, and the zero and pole are shown in Fig. 13.16b. The impedance zero is negative, the pole is positive, and therefore the system is stable.

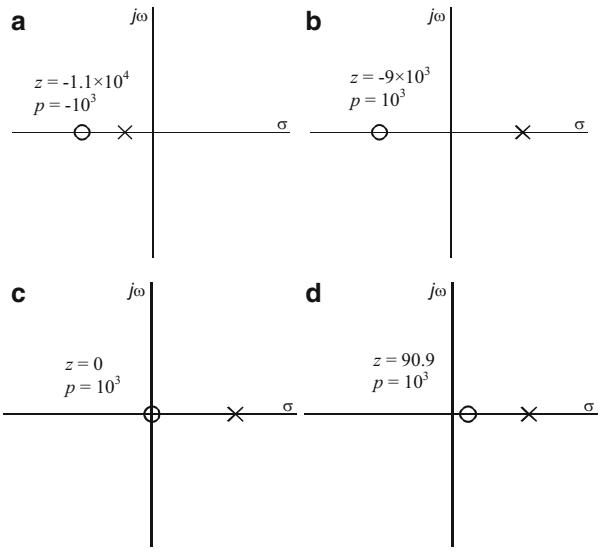

Fig. 13.16 Representation of poles (X) and zeros (O) of impedance on *s*-plane; parameters as in Fig. 13.15; poles, *p*, and zeros, *z*, are in units s^{-1}

When $R_0 = -R_1$, the low-frequency resistance is zero, $R(\omega = 0) = 0$ (Fig. 13.15c). This means that the steady-state current does not perceive any resistance. This leads to a so-called saddle-node bifurcation [588–592]. Such a situation can be obtained for the system in Fig. 13.15b after adding an external resistor in the working electrode connection. A saddle-node bifurcation indicates that there are at least two stationary states and a hysteresis on current-potential characteristics due to nonlinearities in the system exists [590]. Such a behavior is observed, for example, in ethanol oxidation where negative resistances are detected [593, 594]. By adding an external resistance, a sharp peak appears in the reverse sweep of the cyclic voltammograms [595]. The position and shape of this peak are very sensitive to the value of the resistance in the working electrode circuit. At some point, the external resistance compensates the negative low-frequency resistance and the current starts to increase rapidly (Fig. 13.17) [595]. Although at some point the impedance at zero frequency becomes zero, surface conditions change and the current cannot reach infinity.

When $R_0 > -R_1$, both $R(\omega = 0)$ and $R(\omega = \infty)$ are positive, but the direction of the frequencies is opposite to that in Fig. 13.15a. Both the zero and the pole are positive, and the system is unstable.

Let us look at some other examples of a circuit containing a series connection of two (*RC*) elements in parallel and displaying two semicircles, as in Fig. 2.37, left. Let us assume that one resistance related to the low-frequency loop is negative, similar to that shown earlier in Fig. 5.3d for a system with one adsorbed species. An example of the complex plane plots obtained at different values of the resistance R_0 are displayed in Fig. 13.18. The impedance of this circuit is described as

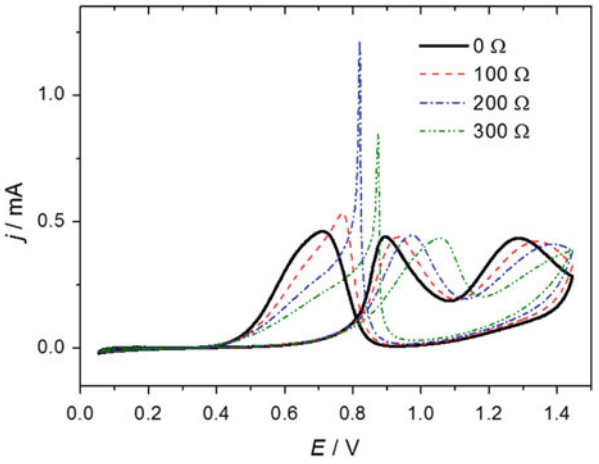

Fig. 13.17 Cyclic voltammograms at Pt in 1 M EtOH and 0.5 M H_2SO_4 measured directly and after adding various resistances to working electrode connection; sweep rate 50 mV s^{-1} (From Ref. [595], copyright (2012), with permission from Elsevier)

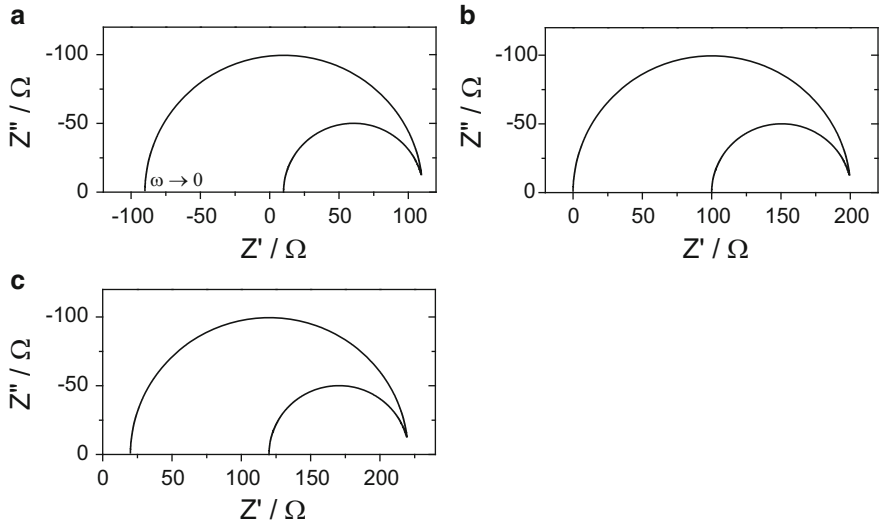

Fig. 13.18 Complex plane plots for circuit $R_0(R_1C_1)(R_2C_2)$ in Fig. 2.37 *left*. Parameters: $R_1 = 100\ \Omega$, $C_1 = 2 \times 10^{-5}$ F, $R_2 = -200\ \Omega$, $C_2 = 0.01$ F; resistance in series R_0: (**a**) 10 Ω, (**b**) 100 Ω, (**c**) 120 Ω

$$\hat{Z} = R_0 + \frac{1}{\frac{1}{R_1} + sC_1} + \frac{1}{\frac{1}{R_2} + sC_2} =$$

$$= \frac{R_0\left[s^2 + s\left[\frac{1}{R_1C_1} + \frac{1}{R_2C_2} + \frac{1}{R_0}\left(\frac{1}{C_1} + \frac{1}{C_2}\right)\right] + \frac{1}{C_1C_2}\left(\frac{1}{R_1R_2} + \frac{1}{R_0R_1} + \frac{1}{R_0R_2}\right)\right]}{\left(s + \frac{1}{R_1C_1}\right)\left(s + \frac{1}{R_2C_2}\right)} \tag{13.26}$$

Table 13.1 Zeros and poles of impedances presented in Fig. 13.18

R_0/Ω	z_1/s^{-1}	z_2/s^{-1}	p_1/s^{-1}	p_2/s^{-1}
10	−5,509	−0.408	−500	0.5
100	−1,000	0	−500	0.5
120	−917	0.0454	−500	0.5

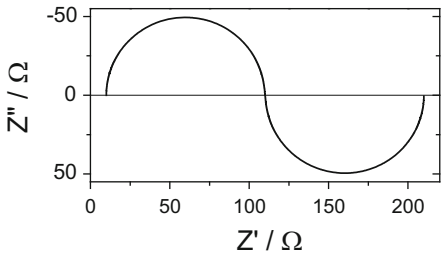

Fig. 13.19 Complex plane plots for circuit in Fig. 2.37 *left*. Parameters: $R_1 = 100\ \Omega$, $C_1 = 2 \times 10^{-5}$ F, $R_2 = 100\ \Omega$, $C_2 = -0.01$ F, $R_0 = 10\ \Omega$

with zeros and poles

$$z_{1,2} = \frac{\frac{1}{R_1C_1} + \frac{1}{R_2C_2} + \frac{1}{R_0C_1} + \frac{1}{R_0C_2}}{2}\left[-1 \pm \sqrt{1 - \frac{\frac{4}{C_1C_2}\left(\frac{1}{R_1R_2} + \frac{1}{R_0R_1} + \frac{1}{R_0R_2}\right)}{\left(\frac{1}{R_1C_1} + \frac{1}{R_2C_2} + \frac{1}{R_1C_1} + \frac{1}{R_0C_2}\right)^2}}\right],$$

$$p_1 = -\frac{1}{R_1C_1} \quad p_2 = -\frac{1}{R_2C_2}. \tag{13.27}$$

Figure 13.18 presents complex plane plots for this model for different values of R_0 and the values of the poles and zeros presented in Table 13.1.

There is always one negative and one positive pole, which are independent of the value of R_0. For the resistance $R_0 = 10\ \Omega$ (Fig. 13.18a) there are two negative zeros, and the system is stable. For $R_0 = 100\ \Omega$ one zero equals zero. In this case, the low-frequency impedance becomes zero, which indicates a saddle-node bifurcation. At $R_0 > 100\ \Omega$, a positive zero appears, and the system is no longer stable.

The last example is of the same model as the preceding one, but with negative capacitance C_2. Its complex plane plot is shown in Fig. 13.19. This system has two zeros: $z_1 = -5.491\ s^{-1}$ and $z_2 = 2.91\ s^{-1}$. Since one zero is positive, this system is always unstable.

Example 13.2 Using the electrical equivalent model $R_0(C_1(R_1(R_2C_2)))$ in Fig. 2.27, check its stability assuming the following parameters: $R_0 = 10\ \Omega$, $C_1 = 10^{-5}$ F, $C_2 = -0.001$ F; and R_2: (a) $-150\ \Omega$, (b) $-110\ \Omega$, (c) $-80\ \Omega$.

Table 13.2 Zeros and poles of impedance in Eq. (13.28) for different values of parameter R_2

R_2/Ω	z_1/s^{-1}	z_2/s^{-1}	p_1/s^{-1}	p_2/s^{-1}
−150	−10,999	2.42	$1.66 - j\,81.6$	$1.66 - j\,81.6$
−110	−10,999	0	$0.449 - j\,95.3$	$0.449 + j\,95.3$
−80	−10,999	−3.41	$-1.25 - j\,112$	$-1.25 + j\,112$

First, the system impedance must be written in the form of Eq. (13.22):

$$Z = R_0 + \cfrac{1}{sC_1 + \cfrac{1}{R_1 + \cfrac{1}{sC_2 + \cfrac{1}{R_2}}}} = R_0 \frac{s^2 + s\left[\frac{1}{C_2}\left(\frac{1}{R_1}+\frac{1}{R_2}\right)+\frac{1}{C_1}\left(\frac{1}{R_1}+\frac{1}{R_0}\right)\right] + \frac{1}{C_1C_2}\left(\frac{1}{R_1R_2}+\frac{1}{R_0R_1}+\frac{1}{R_0R_2}\right)}{\left[s^2 + s\left(\frac{1}{C_2}\left(\frac{1}{R_1}+\frac{1}{R_2}\right)+\frac{1}{R_1C_1}\right)+\frac{1}{R_1R_2C_1C_2}\right]}. \tag{13.28}$$

Its zeros and poles were already presented in Eq. (2.160). The results are presented in Table 13.2 and the impedance plots in Fig. 13.20.

From the results presented it is evident that in case (a), the impedance displays one positive zero, which indicates that this system is unstable; in case (b), the low-frequency zero is equal to zero, which indicates a saddle-node bifurcation; and in case (c), both zeros are negative and poles are complex with negative real part; therefore, the system is stable.

The method presented here allows for the determination of system stability following determination of the system zeros and poles.

13.3.4 Nyquist Stability Criterion

Sometimes we would like to resolve system stability without modeling impedances or determining the zeros and poles of the impedance. This can be done using the Nyquist stability criterion [587, 588, 596] developed from the theory of complex functions and Cauchy's integral theorem, which can be stated as follows: an electrochemical system is stable if and only if the number of clockwise encirclements (#N) of the origin of the $Z' - (-Z'')$ plane, going from low to high frequencies, equals the number of positive poles (#P), i.e., in the right-hand s-plane. Therefore, the number of instabilities, that is, positive zeros, equals $\#Z = \#P - \#N$.

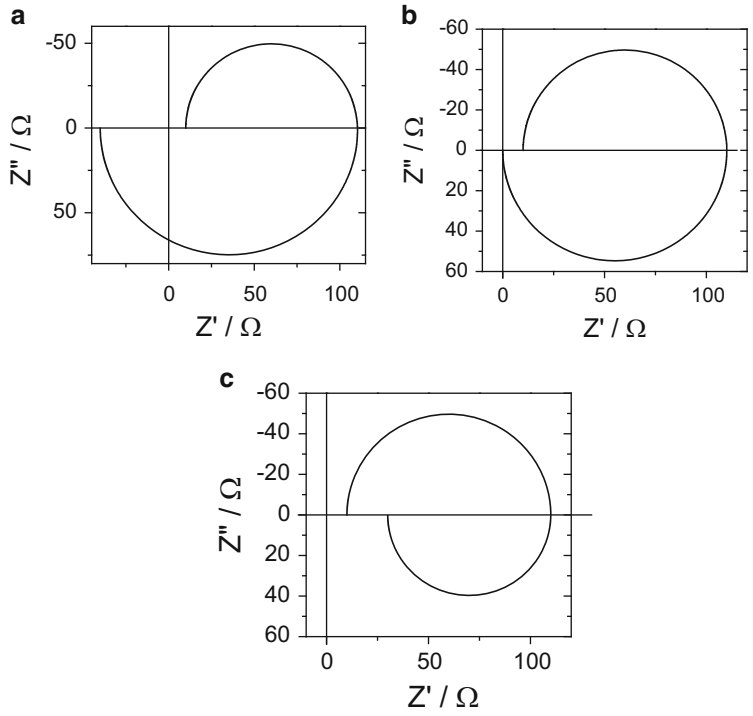

Fig. 13.20 Complex plane plots for model and data in Example 13.2

Let us look at the impedances in Fig. 13.15b–d. They all have a negative resistance and one positive pole, #P = 1, Eq. (13.24). In Fig. 13.15b, going from $\omega = 0$ to $\omega \to \infty$ (that is, from left to right), the origin is circled once, which means that #N = 1 and the number of instabilities #Z = #P − #N = 1 − 1 = 0, and the system is stable. In Fig. 13.15c, the impedance at $\omega = 0$ is $Z = 0$, and a saddle-node bifurcation occurs. In Fig. 13.15d, R_1 is still negative; therefore, #P = 1. The impedance does not encircle the origin, and #N = 0; therefore, the number of instabilities is #Z = #P − #N = 1 − 0 = 1, and this system is unstable.

Let us consider a system containing two parallel (RC) elements in series and displaying two semicircles ($R_0(R_1C_1)(R_2C_2)$, Fig. 2.37, left). Let us assume that the two resistances are negative, and the higher capacitance is negative given different solution resistances R_0. The complex plane plots corresponding to this circuit for negative $R_1 = R_2$, negative C_2, and different values of the serial resistance R_0 are displayed in Fig. 13.21. They will be used for the illustration of the stability criterion. The values of the zeros and poles of the impedances, calculated using Eq. (13.27), are shown in Table 13.3. There is always one positive and one negative pole. For $R_0 < 100\ \Omega$ the impedance zeros are both negative. Going from low to high frequencies there is one clockwise encirclement of the origin, and as there is only one positive pole, there are no instabilities, #Z = #P − #N = 1 − 1 = 0.

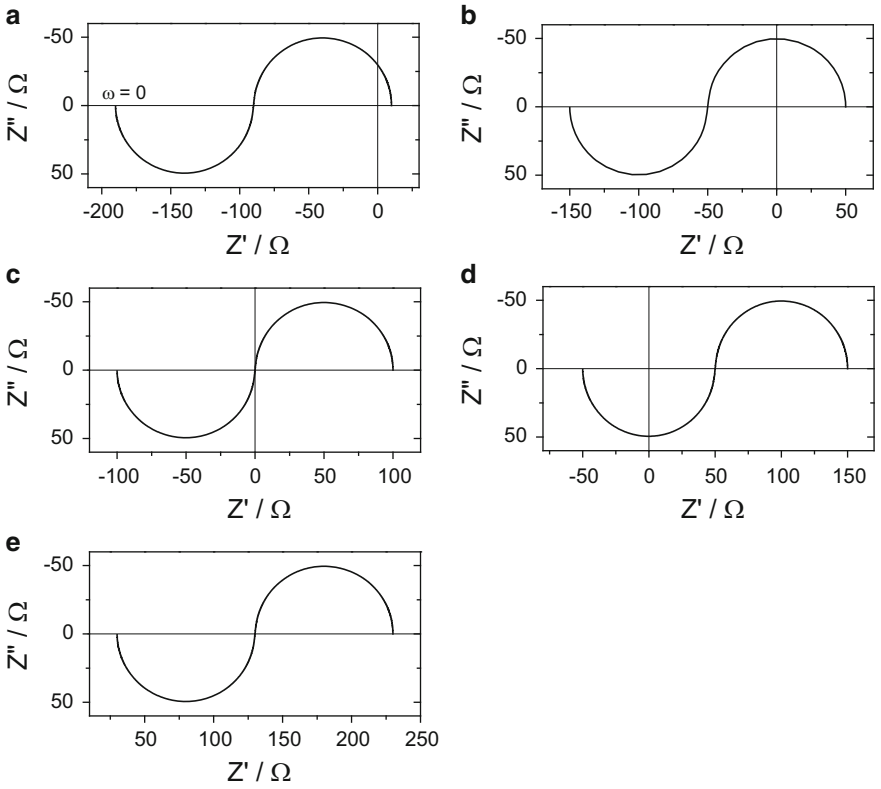

Fig. 13.21 Influence of serial resistance on complex plane plots for circuit in Fig. 2.37 *left*. Parameters: $R_1 = R_2 = -100\ \Omega$, $C_1 = 2 \times 10^{-5}$ F, $C_2 = -0.01$ F, $R_0 =$ (**a**) 10 Ω, (**b**) 50 Ω, (**c**) 100 Ω, (**d**) 150 Ω, (**e**) 230 Ω

Table 13.3 Zeros and poles of impedance defined in Eq. (13.27) for parameters in Fig. 13.21

R_0/Ω	z_1/s^{-1}	z_2/s^{-1}	p_1/s^{-1}	p_2/s^{-1}
10	−4,489	−2.12	500	−1
50	−496	−3.02	500	−1
100	$0 - j\ 22.4$	$0 + j\ 22.4$	500	−1
150	$83.2 - j\ 82.2$	$83.2 + j\ 82.2$	500	−1
230	$141 - j\ 141$	$141 + j\ 141$	500	−1

When $R_0 = -R_2$, there are two complex conjugate zeros with real part equal to zero. On the complex plane plot, for one value of the frequency $\omega_H \neq 0$ the impedance becomes zero. This is a so-called Hopf bifurcation, and the frequency is called a Hopf frequency. At $R_0 > -R_2$, the zeros are complex with positive real part, which indicates instability (Fig. 13.14). In fact, in Fig. 13.21d, there is only a counterclockwise encirclement of the origin, and in case e, there are no encirclements; therefore, on the basis of the Nyquist theorem, the system is unstable.

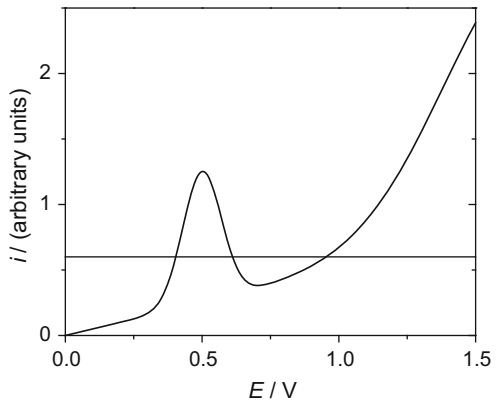

Fig. 13.22 Example of *current-potential curve*; negative resistance may appear when $di/dE < 0$; *parallel line* indicates that multiple states are possible for one value of current

Applying the Nyquist theorem to the impedances in Fig. 13.18 it is evident that in case a, there is a negative low-frequency resistance and one pole is positive. However, the impedance encircles the origin once in the clockwise direction (going from low to high frequencies) and the number of instabilities is $\#Z = \#P - \#N = 1 - 1 = 0$; therefore, the system is stable. Other cases can be considered in a similar way.

13.3.5 Negative Dynamic Resistances and Their Origin

Negative impedance cannot be read from the steady-state polarization curve. However, in dynamic systems, for example, during a voltamperometric potential sweep, such effects can appear. These phenomena are often observed in corrosion in cases of active-passive transitions or transpassivity [588–600]. An example of the $i-E$ curve where negative charge transfer resistances are observed is displayed in Fig. 13.22 (see also Refs. [599, 600]); they appear after the peak where the current is decreasing with increasing potential, $di/dE < 0$. It should also be noted that during potentiostatic experiments, one current value corresponds to one potential, whereas for one applied current (galvanostatic conditions) (horizontal line) three values of the current are possible because of multiple steady states.

Koper [597], Koper and Sluyters [598], and Krischer and Varela [601] discussed the conditions under which negative faradaic impedance can be observed. In general, current is described as

$$i_f = nFAk_fC(0), \tag{13.29}$$

where A is the electrode surface area, $C(0)$ is the surface concentration of the electroactive species, and other parameters have their usual meaning. Faradaic admittance is defined as

$$\hat{Y}_{\mathrm{f}} = \frac{1}{\hat{Z}_{\mathrm{f}}} = \frac{\mathrm{d}i_{\mathrm{f}}}{\mathrm{d}E} = nF\left[AC(0)\frac{\mathrm{d}k_{\mathrm{f}}}{\mathrm{d}E} = Ak_{\mathrm{f}}\frac{\mathrm{d}C(0)}{\mathrm{d}E} + k_{\mathrm{f}}C(0)\frac{\mathrm{d}A}{\mathrm{d}E}\right]. \tag{13.30}$$

To obtain a negative faradaic impedance, the expression in parentheses in Eq. (13.30) must be negative. This can happen in one of three cases [597, 598]:

i. $\mathrm{d}k_{\mathrm{f}}/\mathrm{d}E < 0$: this condition may occur in the following situations:

   (a) During potential-dependent adsorption of an inhibitor, which decreases the available free surface area. For example, one can assume that the heterogeneous rate constant changes according to

$$k_{\mathrm{f}}(\theta, E) = [1 - \theta(E)]k_{\mathrm{f}}(\theta = 0, E) + \theta(E)k_{\mathrm{f}}(\theta = 1, E), \tag{13.31}$$

   where θ is the surface coverage with the inhibitor and $k_{\mathrm{f}}(\theta = 0, E) >> k_{\mathrm{f}}(\theta = 1, E)$.

   (b) During potential-dependent desorption of a catalyst in whose presence a reaction can proceed at a high rate. When the catalyst is desorbed, the reaction rate decreases with the potential.

ii. $\mathrm{d}C(0)/\mathrm{d}E < 0$: this condition occurs during strong electrostatic repulsion of ions in the double layer due to the Frumkin effect [17]. This effect is especially strong at low supporting electrolyte concentrations as the value of the potential in the outer Helmholtz plane becomes large (positive or negative for cations and anions, respectively).

iii. $\mathrm{d}A/\mathrm{d}E < 0$: this effect can appear when the available electrode surface decreases with increasing polarization due to the formation of a passivating or strongly inhibiting film (potential-dependent processes).

As we saw earlier, systems with a negative faradaic resistance, such as in Fig. 13.15, may be stable, depending on the value of the solution resistance. However, such impedance is not Kramers-Kronig-transform compliant. This is related to the general characteristics of transfer functions. However, there are two types of impedance experiments: potentiostatic or galvanostatic. When an ac voltage is applied and ac current measured, the corresponding transfer function (Laplace transform of the output to the Laplace transform of the input) is admittance,

$$\hat{Y}(\omega) = \frac{L[output]}{L[input]} = \frac{L[i(t)]}{L[E(t)]}, \tag{13.32}$$

and when ac current is used as a perturbation, the transfer function is impedance,

$$\hat{Z}(\omega) = \frac{L[E(t)]}{L[i(t)]}. \tag{13.33}$$

This means that *if the data were acquired under a potentiostatic perturbation, then one should use the admittance as the transfer function* for the Kramers-Kronig

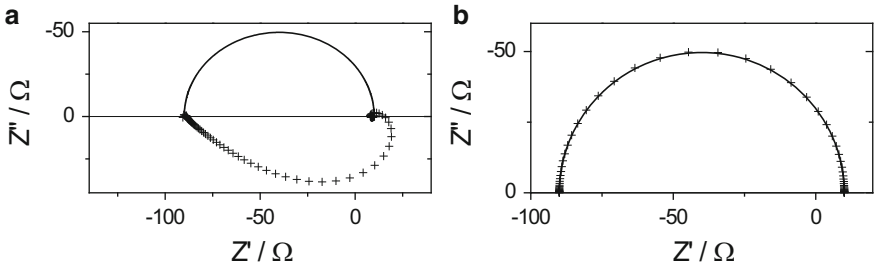

Fig. 13.23 Complex plane impedance data (*continuous lines*) and their Kramers-Kronig transformations (*symbol* +) for simple model with negative resistance; (**a**) transformation of impedance, (**b**) transformation of admittance (displayed here as impedance); data as in Fig. 13.15b

transformations, but *if the data were acquired under a galvanostatic perturbation, then one should use impedance* [561]. This fact is related to system stability. Although it is possible to acquire data using potentiostatic control, during galvanostatic control multiple states are possible for one value of current (Fig. 13.22), and oscillations might be observed [588, 599, 600]. In fact, for a system displaying negative resistance, as in Fig. 13.15b, impedances are not Kramers-Kronig compliant, but admittances are transformable. This result is displayed in Fig. 13.23.

These properties are understandable from the point of view of the stability of transfer functions. As was mentioned earlier, a stable transfer function cannot have any positive poles. In the foregoing case, the poles and zeros of the impedance are shown in Fig. 13.16b, and there is one positive pole and one negative zero, which means that the system is unstable. On the other hand, the admittance (inverse of impedance) has one negative pole and one positive zero, indicating that it is stable. Of course, systems containing only positive R, C, and L elements always have negative poles and zeros, and they are always stable and transformable in the admittance and impedance forms.

Example 13.3 Determine the current and impedance of a system displaying negative impedance (described below). It represents the irreversible metal dissolution and electrosorption of a species A on the surface, which block metal dissolution:

$$\mathrm{M_s} \xrightarrow{k_{1\mathrm{f}}} \mathrm{M^+} + e, \tag{13.34}$$

$$\mathrm{A^-} \underset{k_{2\mathrm{b}}}{\overset{k_{2\mathrm{f}}}{\leftrightarrows}} \mathrm{A_s} + e. \tag{13.35}$$

Use the following parameters: $k_1^0 = k_2^0 = 10^{-7}$ mol cm^{-2} s^{-1}, $\alpha_1 = \alpha_2 = 0.5$, $\sigma_1 = 210\ \mu$C cm^{-2}, $E = 0.1$ V; neglect the diffusion of A$^-$.

Reactions (13.34) and (13.35) are described by the following equations:

$$v_1 = k_{1f}(1-\theta), \tag{13.36}$$

$$v_2 = k_{2f}(1-\theta) - k_{2b}\theta, \tag{13.37}$$

where the rate constants are potential dependent:

$$k_{1f} = k_1^0 \exp(\alpha_1 fE);\ \ k_{2f} = k_2^0 \exp(\alpha_2 fE);\ \ k_{2b} = k_2^0 \exp[-(1-\alpha_2)fE]. \tag{13.38}$$

First, the steady-state conditions must be described. At a steady state, adsorption of species A is in equilibrium and $v_2 = 0$ and the surface coverage is

$$\theta = \frac{k_{2f}}{k_{2f} + k_{2b}}, \tag{13.39}$$

and the steady-state current is

$$i = Fv = F(v_1 + v_2) = F\frac{k_{1f}k_{2b}}{k_{2f} + k_{2b}}. \tag{13.40}$$

Next, the dynamic conditions must be solved. In general, the total ac current is written as

$$\Delta i = \left(\frac{\partial v}{\partial E}\right)\Delta E + \left(\frac{\partial v}{\partial \theta}\right)\Delta\theta, \tag{13.41}$$

where for each parameter a, $\Delta a = \tilde{a}\exp(j\omega t)$. This can be simplified to

$$\tilde{i} = F\left[\left(\frac{\partial v}{\partial E}\right)\tilde{E} + \left(\frac{\partial v}{\partial \theta}\right)\tilde{\theta}\right]. \tag{13.42}$$

The adsorption reaction for reaction (13.35) is

$$\Gamma_\infty \frac{\mathrm{d}\theta}{\mathrm{d}t} = v_2 = k_{2f}(1-\theta) - k_{2b}\theta, \tag{13.43}$$

where Γ_∞ is the maximum surface concentration of the adsorbed species and can be expressed in terms of the maximal charge density necessary for full surface coverage, $\Gamma_\infty = \sigma_1/F$. The linearized form is

$$\Gamma_\infty j\omega\tilde{\theta} = \left(\frac{\partial v_2}{\partial E}\right)\tilde{E} + \left(\frac{\partial v_2}{\partial \theta}\right)\tilde{\theta}. \tag{13.44}$$

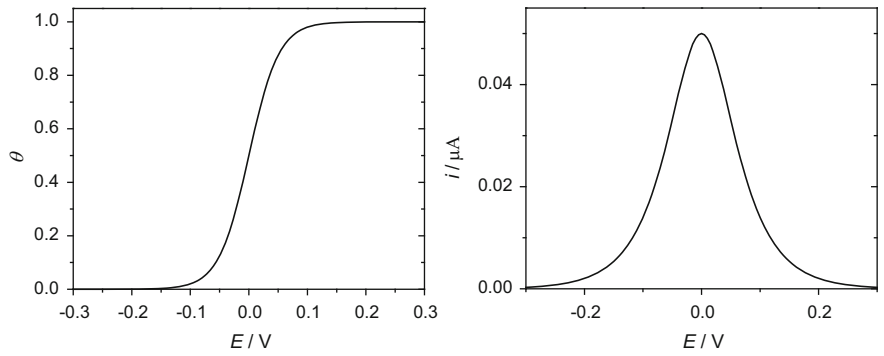

Fig. 13.24 Dependence of surface coverage and current on potential

Equations (13.42) and (13.44) may be written in matrix form:

$$\begin{bmatrix} -\left(\frac{\partial v}{\partial E}\right) \\ -\left(\frac{\partial v_2}{\partial E}\right) \end{bmatrix} = \begin{bmatrix} -\frac{1}{F} & \left(\frac{\partial v}{\partial \theta}\right) \\ 0 & \left(\frac{\partial v_2}{\partial \theta} - j\omega\frac{\sigma_1}{F}\right) \end{bmatrix} \begin{bmatrix} \widetilde{i} \\ \widetilde{E} \\ \widetilde{\theta} \\ \widetilde{E} \end{bmatrix}. \tag{13.45}$$

One notices the analogy to cases involving one adsorbed species. The system faradaic admittance is easily obtained from Eq. (13.45):

$$\widetilde{Y}_\mathrm{f} = F\left[\left(\frac{\partial v}{\partial E}\right) + \frac{\left(\frac{\partial v}{\partial \theta}\right)\left(\frac{\partial v_2}{\partial E}\right)}{\left(\frac{\partial v_2}{\partial \theta}\right) - j\omega\frac{\sigma_1}{F}}\right] = F\left(\frac{\partial v}{\partial E}\right) + \frac{\frac{-F^2}{\sigma_1}\left(\frac{\partial v}{\partial \theta}\right)\left(\frac{\partial v_2}{\partial E}\right)}{j\omega - \frac{F^2}{\sigma_1}\left(\frac{\partial v_2}{\partial \theta}\right)} \tag{13.46}$$

$$= A + \frac{B}{j\omega + C}.$$

This equation is similar to that used for one adsorbed species, Eq. (5.51), and $A = 1/R_\mathrm{ct}$. The total impedance must include a solution resistance and double-layer capacitance,

$$\hat{Z} = R_\mathrm{s} + \frac{1}{j\omega C_\mathrm{dl} + \frac{1}{Z_\mathrm{f}}}, \tag{13.47}$$

and it displays two semicircles on the complex plane plot. Results of the calculations might be easily obtained using Maple/Mathematica. The dependence of the surface coverage and current on the potential is displayed in Fig. 13.24 and the total

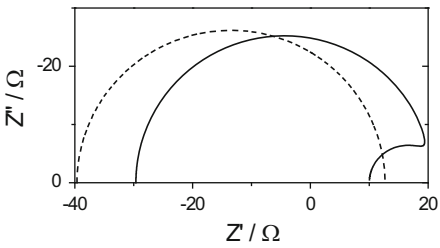

Fig. 13.25 Complex plane plots of total (*continuous line*) and faradaic (*pointed line*) impedances at $E = 0.1$ V

and faradaic impedances in Fig. 13.25. At negative potentials, two semicircles are observed on the complex plane plots, whereas at positive potentials, where the current is decreasing, negative resistance corresponding to a low-frequency loop appears. Such plots were predicted for the case with one adsorbed species (Fig. 5.3).

13.4 Z-HIT Transform

Kramers-Kronig transforms require integration over frequencies from zero to infinity, which, in practice, is difficult to carry out. There exists a Hilbert logarithmic transform [602, 603] that can be used to validate impedance data in a limited frequency range. It is known under the name Z-HIT transform [585] and is used in the Zahner software [604]. The logarithm of a transfer function known for frequencies between ω_s and ω_o may be written as a function of the phase angle:

$$\ln\left|H(\omega_0)\right| = \ln\left|H(0)\right| + \frac{2}{\pi}\int_{\omega_s}^{\omega_0} \varphi(\omega)\ \mathrm{d}\ln\omega + \sum_{k\geq 1,\, k\,\mathrm{odd}} \gamma_k \frac{\mathrm{d}^k\varphi(\omega_0)}{(\mathrm{d}\ln\omega)^k},$$

$$\gamma_k = -\frac{2}{\pi}\zeta(k+1)2^{-k} \quad \text{for odd}\ \ k, k \geq 1;\ \ \zeta(s) = \sum_{n=1}^{\infty} n^{-s}. \tag{13.48}$$

This series may be simplified to

$$\ln\left|H(\omega_0)\right| \approx const + \frac{2}{\pi}\int_{\omega_s}^{\omega_o} \varphi(\omega)\ \mathrm{d}\ln\omega + \gamma\frac{\mathrm{d}\varphi(\omega_o)}{\mathrm{d}\ln\omega}, \tag{13.49}$$

where $\gamma = -\pi/6$. Equation (13.49) indicates that the logarithm of the transfer function may be calculated from the integral and the derivative of the phase angle [585] and presents an alternative to the Kramers-Kronig transform.

Application of the coherence function instead of the classical Kramers-Kronig transforms has also been proposed in the literature [37, 605] but is rarely used in practice.

13.5 Summary

Experimental impedance data should be validated before further analysis. Raw data might be verified using Kramers-Kronig or Z-Hit transforms. It should be kept in mind that these transforms are not very sensitive to system nonlinearities, and an additional test with different amplitudes could be carried out. An alternative to the aforementioned transforms is the approximation to linear circuits (Figs. 13.2 and 13.4).

If approximation by the transfer function in the form of Eq. (13.17) is possible, then poles of the transfer function can be analyzed because the stable transfer function cannot have positive poles. When such an analysis is not possible, one can use the Nyquist stability criterion. Only validated data can be used for analysis.

13.6 Exercises

Exercise 13.1 Carry out a K-K transform of the data in the file 1.z.
Exercise 13.2 Carry out a K-K transform of the data in the file 2.z.
Exercise 13.3 Carry out a K-K transform of the data in the file 3.z.
Exercise 13.4 Perform a K-K transform of the data in the file 4.z.
Exercise 13.5 Perform a K-K transform of the data in the file 5.z.